Moroccan Journal of Chemistry
ISSN : 2351-812X

Mor. J. Chem., 2023, Volume 11, Issue 02, Page 333-349
https://revues.imist.ma/index.php/morjchem

The adsorptive potential of potassium hydroxide treated water lily leaves for malachite green dye removal from aqueous solution: isotherms, kinetics and thermodynamics studies

Abdulmumini H. [1], Ayuba A. M. [2*]

[1] *Department of Science Laboratory Technology, School of Science and Technology, Tatari Ali Polytechnic, PMB 0094, Bauchi, Nigeria*

[2]*Department of Pure and Industrial Chemistry, Faculty of Physical Sciences, Bayero University, P. M. B. 3011, Kano, Nigeria*

**Corresponding author, Email address: ayubaabdullahi@buk.edu.ng*

Received *08 July 2022,*
Revised *13 Feb 2023,*
Accepted *19 Feb 2023*

Citation*: Abdulmumini H., Ayuba A. M., (2023) The Adsorptive potential of potassium hydroxide treated water lily leaves for malachite freen gye removal from aqueous solution: Isotherms, kinetics and thermodynamics studies, Mor. J. Chem., 14(2), 333-349. Doi: https://doi.org/10.48317/IMIST.PRSM/morjchem-v11i1.33392*

Abstract: In this research work, a chemically treated water lily leaves (AWL) powder was prepared and used as low cost, efficient and environment friendly adsorbent for the removal of Malachite green (MG) from aqueous solution. Physical parameters of this adsorbent including moisture content (9.93%), ash content (9.09%), organic matter (90.91%), bulk density (0.316g/cm^3), pore volume (1.89cm^3) and pH (7.07) were determined using standard methods. The adsorbent was characterized by Fourier Transform-Infrared Spectroscopy (FT-IR), Point of Zero Charge (PZC) and Scanning Electron Microscopic (SEM) methods to determined its surface functional group, net neutral charge of 5.90 and surface morphology respectively. Batch techniques were employed to optimize various operational parameters such as contact time, adsorbent dosage, initial dye concentration, solution pH and temperature respectively. The percentage adsorption and adsorption capacity were found to be 90.66% and 148.83mg/g respectively. The kinetics data analyzed were best fitted into pseudo-second order relative to other models tested (pseudo-first order, Elovich and Intraparticle diffusion Models) for the different operating temperatures (30, 40, 50^{0}C). The isotherms were estimated and confirmed to best fit into D-R model compared to Langmuir, Freundlich and Temkin models analyzed. Thermodynamics studies indicates that the sorption is spontaneous, exothermic, and decrease in randomness of the system during the adsorption process as a results of negative values for Gibb's Free energy (ΔG), enthalpy (ΔH), and Entropy (ΔS). This study confirmed that chemically treated water lily leaves (AWL) powder could be used as an alternative adsorbent for removal of toxic dyes such Malachite green.

Keywords: Water lily leaves; Malachite green; Thermodynamics; Kinetics; Adsorption; Isotherms

1. Introduction

With the advent of new and sophisticated technologies in the manufacture and processing of goods, problems associated with an increase in discharge of deleterious materials and subsequent pollution of the ecosystem is inevitable (Elsherif *et al*., 2022). Dye pollution is one of the major problems faced by many countries around the world due to an increase in unregulated industrial activities in their domain. These industries release dye containing effluents as pollutants which

causes significant health hazards to living organisms and overall detritions to the environment (Kali *et al*., 2022). The major problem concerning the environmental protection is pollution of wastewaters with pesticides, dyes, heavy metals etc (Marczewski *et al*., 2016). Water pollution by dyes is believed to begin during the earliest use of colorants by Neanderthal man about 180,000 years ago (Erradi and Jaafari, 2022). However, modern pollution of water by dyes could be tracked back to the years that followed the discovery of first synthetic dye.

Adsorption is the simplest and easiest treatment method for contaminated effluent water compared to the other methods available (Tcheka *et al*., 2021). This process involves the use of certain substances which concentrate specific substances from solution onto their surface (Oznur *et al*., 2013). Various low-cost adsorbents that have been employed for the adsorption of dyes from aqueous solution or wastewater include orange peels (Elsherif *et al*., 2022), maize cob (Ojediran *et al*., 2021), chitosan (Monvisade and Siriphannon, 2009), modified agricultural bye-product (Sciban *et al*., 2008), natural and modified clay minerals (Crini, 2006), Maize cob (Ibrahim and Jimoh, 2008; 2012), activated carbon obtained from *cordia myxa* (Kihc and Janabi, 2017), Orange peel (Mafra *et al*., 2013), Banana stalk (Bello *et al*., 2012), Nymphaea alba (Zendegani and Shokrollahi, 2014), Composite Based on Hydroxyapatite/Hydroxypropyl Methyl-Cellulose (Kankou *et al*., 2021), Activated Carbon (Kankou *et al*., 2021) among others.

Therefore, in this study potassium hydroxide (KOH) treated water Lily leaves (AWL) powder was used to investigate its adsorption capacity for MG removal from aqueous solutions. The effects of various parameters such as contact time, adsorbents dosage, initial dye concentration, pH of the solution and temperature in relation to the adsorption process of MG were studied using batch experimental techniques. The kinetic and isotherms models of MG adsorption onto AWL were analyzed through pseudo-first order, pseudo second order, Elovich, intraparticle diffusion kinetic models and Langmuir, Freundlich, Temkin and D-R isotherm models respectively. Thermodynamics studies were conducted in order to determine changes in Gibb's free energy, enthalpy and entropy of the adsorption process. Some physical parameters of AWL were also successfully evaluated.

2. **Methodology**

2. Materials and methods

2.1 Sample collection and adsorbent preparation

The water lily leaves (WLL) were obtained from Gubi Dam, Bauchi State, Nigeria. The leaves were washed thoroughly with distilled water and shade dried for 72hours. The adsorbent was prepared according to a method reported by Amode *et al.* (2016). The dry leaves were ground to powder and 10g sample was treated with 100ml solution of 1.0M KOH in a beaker. The mixture was stirred thoroughly with magnetic stirrer and then allowed to age for 24h prior to achieve good penetration of the chemical into the interior of the adsorbents (precursor). The sample was then washed severally with 0.1M HCl to neutralize excess KOH and finally with hot distilled water severally. The resultant sample was air dried, ground and sieved to a working size of 300µm and stored in air tight polythene bottles, labeled as AWL for further use.

2.2 The physicochemical analysis of the adsorbent

2.2.1 Determination of ash and moisture contents

The ash and moisture contents were determined by weight difference (Gaya *et al*., 2015). For moisture content, 1g of AWL was placed in a crucible and heated continuously at 105ºC for 3 hours in an electric oven then cooled in desiccator and weighed. The procedure was repeated several times

at the same temperature for 15 min interval until constant weights were obtained. The percentage moisture content of the sample was determined using **Eqn. 1**.

$$\%\text{Moisture content} = \frac{W_1 - W_3}{W_2 - W_1}\ x\ 100 \qquad \text{Eqn. 1}$$

Where, w_1 is weight of empty crucible, w_2 is weight of crucible and the sample after heating, w_3 final weight of the crucible containing the sample after heating.

In the determination of ash content, 1g or AWL was placed in a crucible of known weight and then heated at 500^0C for 3 hours. The sample was cooled in a desiccator and weighed. The ash content of each sample was calculated from the weight of the sample before and after heating using **Eqn. 2**:

$$\%\text{Ash content} = \frac{W_1 - W_3}{W_2 - W_1}\ x\ 100 \qquad \text{Eqn. 2}$$

Where, w_1 is the initial weight of crucible, w_2 is initial weight of the crucible containing the sample before heating and w_3 is the final weight of crucible containing the ash sample.

2.2.2. Determination of organic matter content

The organic matter content of the AWL adsorbent was determined from the difference between 100% air-dried AWL adsorbent determined and the percentage ash content (Ayuba and Nyijime, 2021) as illustrated in **Eqn. 3**:

$$\%\ \text{Organic matter content} = 100 - \%Ash\ content \qquad \text{Eqn. 3}$$

2.2.3 Determination of pH

1g of the AWL sample was put inside a 250ml Erlenmeyer flask. Then 100ml of distil water was poured into the flask. The solution was heated for 15minutes in a boiling condition. The solution was cooled at room temperature and diluted with distilled water to 100ml. the solution was stirred well and the pH was determined using pH meter (Nyijime *et al*., 2021).

2.2.3 Determination of pore (void) volume

In order to determine the pore volume of the AWL adsorbent, a method reported by Ayuba and Nyijime (2019) was adopted. 2.0g of the samples (AWL) was immersed in water and boiled for 15min till the air in the pores had been displaced. The sample was then dried superficially and reweighted. The difference in weight is divided by the density of water gave the pore volume.

$$\text{Pore (void)volume} = \frac{W_2 - W_1}{density\ of\ water} \qquad \text{Eqn. 4}$$

Where, w_1 is the weight of the sample after boiling, w_2 is the weight of the sample before boiling and the density of water is $1g/cm^3$.

2.2.4 Determination of bulk density (apparent density)

The bulk density of the sample was determined so as to know the packed density of a sample. Its carried out according to Giwa *et al.* (2018) and Ayuba and Nyijime (2019). The bulk density of AWL was determined using Archimedes' principle by weighing $10cm^3$ measuring cylinder before and after filling with the AWL samples. The measuring cylinder was then dried and the sample was packed inside the measuring cylinder, leveled and weighed. The weight of the sample packed in the

measuring cylinder was determined from the difference in weight of the filled and empty measuring cylinder. The volume of water in the container was determined by taking the difference in weight of the empty and water filled measuring cylinder. The bulk density was determined using the **Eqn. 5**:

$$\text{Bulk density} = \frac{W_2 - W_1}{V} \qquad \textbf{Eqn. 5}$$

Where w_1 is weight of empty measuring cylinder, w_2 is weight of cylinder filled with AWL sample and V is volume of the cylinder.

2.2.5. Determination of point of zero charge (PZC)

The pH drift method was adopted according to Nasiruddin and Sarwar (2007). The pH of 0.01 NaCl was adjusted to a value between 2 and 11 using 0.50M HCl or 0.50M NaOH. 0.10g of AWL was added to the 50ml of the adjusted solution in a capped vial and equilibrated for 24hours. The final pH was measured and plotted against initial pH. The pH at which the curve intercepts the pH line was taking as point of zero charge.

2.2.6 FT-IR analysis

Fourier transform infrared spectroscopy was used to study the surface functional groups of the adsorbent. FT-IR spectra were obtained with a type spectrum 100 series FTIR spectrometer (Agilent Technology Perkin Elmer Spectrum 100, USA) using the transformation of 20 scans with spectral resolution of $4cm^{-1}$ by attenuated total reflectance method. FTIR spectra were collected in the mid infrared region between 4,000 and $650cm^{-1}$. Spectra were acquired using air background correction (Anisuzzaman *et al*., 2014).

2.2.7 Scanning electron microscopic (SEM) analysis

Scanning electron microscope (SEM) is an analysis of surface morphology of the adsorbent which was carried out by viewing the electron micrographs of the materials (Sartape *et al*., 2017). Analysis was done with proxy Scanning Electron Microscope (Phenom world Eindhoven). In sample preparation for the SEM analysis, a thin layer of adhesive serving as carbon glue was attached onto a stub, and very small amount of the materials to be view was spread on the stub materials and subsequently viewed in the instrument to obtain micrographs. Scanned micrographs of AWL before and after adsorption were taking at an accelerating voltage of 15.00kV and 1500X magnification respectively.

2.3 Preparation of dye stock solution

Stock solution of Malachite green dye (**Figure 1**) was prepared by dissolving 1g of dye in 1000ml volumetric flask at room temperature and shaken until homogenous solution was obtained (Ibrahim and Sani, 2015). The sample of required concentration were prepared by diluting the stock solution with distil water to a required concentration using dilution formula shown in **Eqn. 6**.

$$C_1V_1 = C_2V_2 \qquad \text{Eqn. 6}$$

Where C_1, C_2, V_1 and V_2 are the initial and final concentrations and volumes of the solution.

The concentration of residual the un-adsorbed MG dye was measured at working wavelength (λmax =615.50nm) using UV-visible spectrophotometer (Hitachi 2800 model).

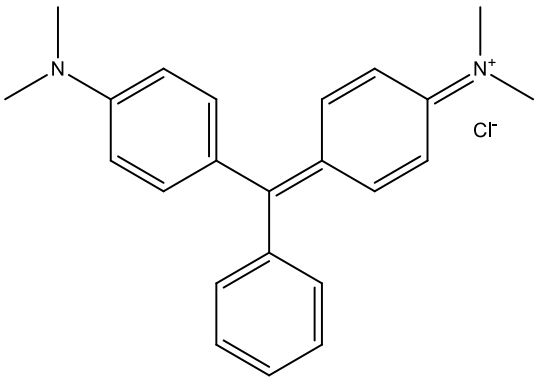

Figure 1. Structure of Malachite Green.

2.4. Adsorption equilibrium experiments

For this experiment, the batch adsorption was adopted because of its simplicity (Shahryari *et al*., 2010). The batch experiments were carried out to determine the optimum conditions for equilibrium adsorption of MG dye onto AWL adsorbent. The results obtained after optimization experiments (90min agitation period, 0.02g adsorbent dosage, 100ppm concentration, 11 pH of solutions) were used to conduct the batch adsorption experiments. This system was run in a 60cm^3 polythene sample bottles at 30, 40, 50 and 60^{0}C temperature respectively. The samples were placed in temperature controlled shaker for the period reported. After reaching equilibrium period, the content was filtered and the filtrate was analyzed using Perkin-Elemer UV-visible Spectrophotometer at maximum absorbance wavelength of 615.4nm. The amount of the adsorbed dye was obtained using **Eqn. 7**:

$$Q_e = \frac{(C_o - C_e)}{m} x\ V \qquad \text{Eqn. 7}$$

While colour removal rate (%Removal) was calculated using **Eqn. 8**:

$$\%R = \frac{(C_o - C_e)}{C_o}\ x\ 100 \qquad \text{Eqn. 8}$$

Where: Q_e is adsorption capacity (mg/g), C_o and C_e are the initial and final concentrations in (mg/l) respectively for the dye in the solution, V is the volume of the dye in solution (L) and m is the mass of the adsorbent (Shahryari *et al*., 2010; Ibrahim and Sani, 2015).

3. Results and Discussion

3.1 Physical analysis of the adsorbent

The physical properties of the adsorbent produced and analysed are presented in Table 1. The results reported are in form of mean±standard deviation of the triplicate analysis. The low value of the moisture content, high pore volume and organic matter of the studied adsorbent revealed that it had good adsorptive properties. Similar results were reported by Ayuba and Thomas (2019) for their study on the physical properties of carbonised Bambara groundnut (*Vigra subterranean*) shells.

Table 1. The physical properties of AWL adsorbent

Moisture Content (%)	Ash Content (%)	Organic Matter (%)	pH	Pore Volume (cm^3)	Density (g/cm^3)
9.93±0.39	9.09±0.25	90.91±0.25	7.07±0.13	1.89±0.21	0.316±0.03

3.2 Characterization of the adsorbent

The FT-IR spectra of the adsorbent (**Figure 2**) before and after adsorption shows some changes in the observed peaks and the various functional group are enumerated in **Table 2**. After the adsorption, there was broadening and shift of the adsorption peaks. The shift of O-H, C-H, COOH group, C=C aromatics, C-O stretch and C-H aromatics vibration from 3436 to 3309cm^{-1}, 2922 to 2981cm^{-1}, 1406 to 1514cm^{-1}, 1325 to 1369cm^{-1} and 1032 to 1026cm^{-1} respectively indicating the participation of functional group in the adsorption process of MG onto AWL. The shifting or splitting of some peaks after adsorption process indicates chemical interaction taking place between the adsorbents and the dyes (**Nasiruddin and Sawar, 2007**).

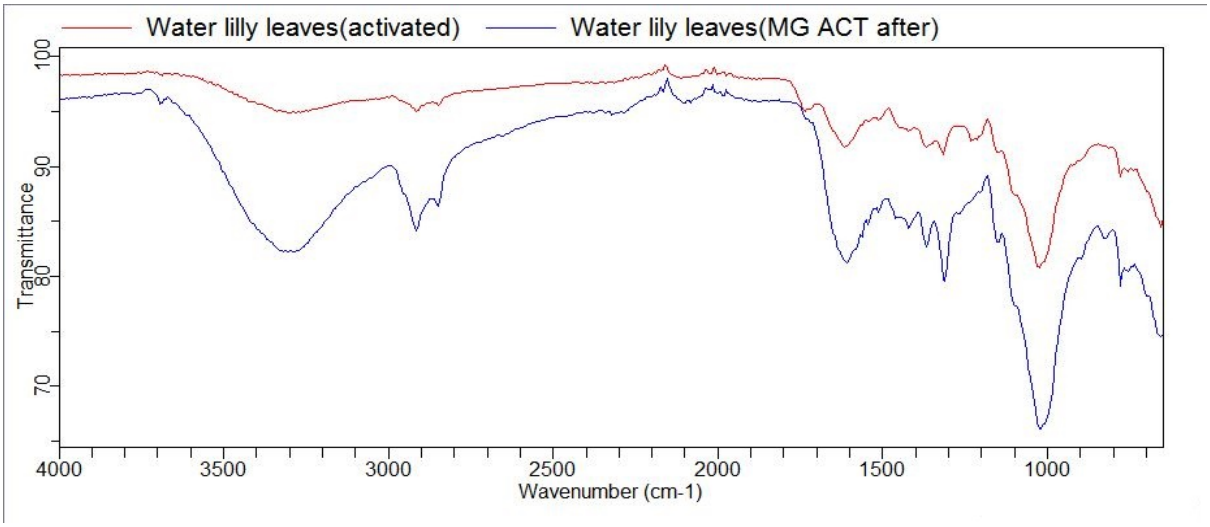

Figure 2. FTIR spectrum of AWL before and after adsorption of MG dye

Table 2. Functional group recognised before and after adsorption of MG and MV onto AWL.

Functional group	Wavelength range (cm^{-1})	Before (cm^{-1})	After (cm^{-1})	Difference (cm^{-1})
O-H stretch	3300-3400	3436	3309	127
C-H stretch	2850-2960	2922	2918	4
COOH group	1690-1760	1632	1611	21
C=C aromatics	1500-1700	1406	1514	108
C-O stretch	1080-1300	1325	1369	44
C-H aromatics	675- 1050	1032	1026	6

The SEM is an analytical tool used for evaluating the surface characteristics of the adsorbent material. The SEM micrographs of AWL adsorbent (**Figures 3a-3b**) shows a surface morphology to be rough, heterogeneous, with irregular defects, cracks and cavities. After adsorption, the crack had widened and the porous structures are filled with deposits of adsorbed MG dyes molecules. These changes observed after adsorption confirmed the binding of the dye molecule onto the functional group moieties present on the surface of AWL adsorbent. The pH_{zpc} of the adsorbent is a very important characteristic that determined the pH at which the adsorbent surface has net electrical neutral charge (Makeswari and Santhi, 2013). **Figure 4** shows the plot of point of zero charge (pH_{zpc}) for AWL adsorbent. The point of zero charge of AWL is found to be 5.90. The adsorbent has a perfect charge balance in acidic regions whereas the acidic water donates more hydrogen ions than hydroxyl ions and the surface of these adsorbents are positively charge and can possible attract the anion substances.

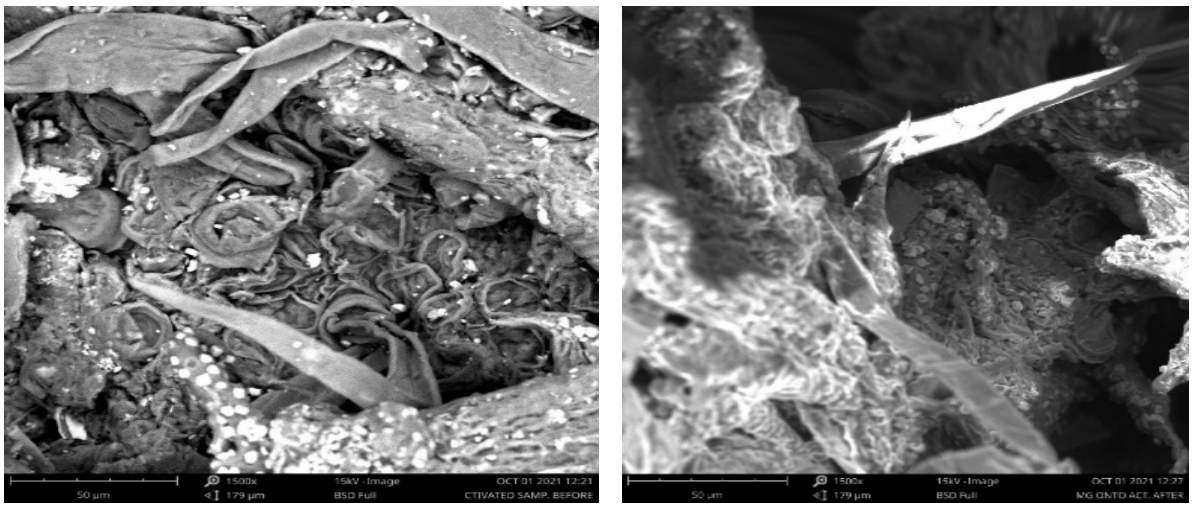

(a) (b)

Figure 3. SEM Micrographs for AWL Sample (a) Before adsorption (b) After adsorption

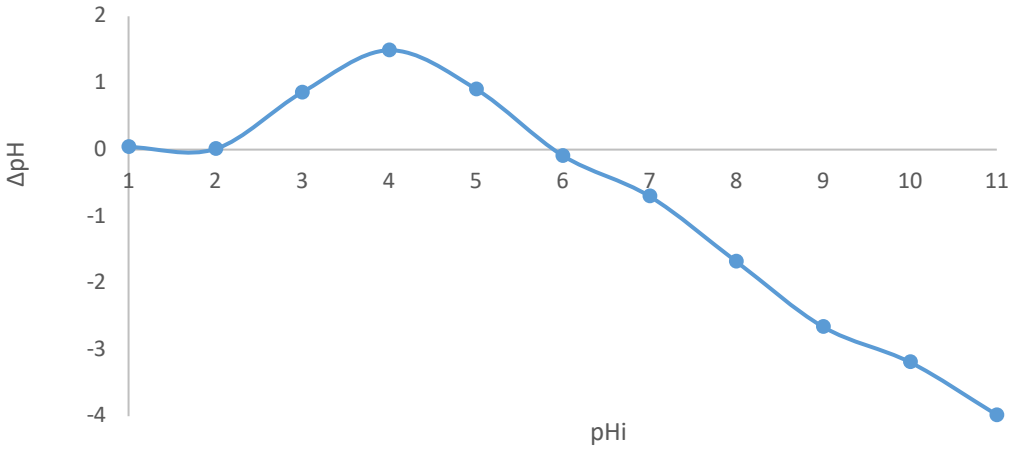

Figure 4. Point of Zero charge (pH_{pzc}) for AWL adsorbent

3.3 The batch adsorption

The effect of contact time for the adsorption of MG onto AWL was studied by varying the contact time from (5-150min). The agitation time is an important factor that affects all transfer phenomena such as adsorption process. According to Suyambo and Perumal (2012) with increased agitation time, the diffusion rate of dye molecules from bulk liquid to the liquid-adsorbents interphase become higher due to enhanced turbulence and decrease thickness of the interphase layer. The fast sorption recorded at the beginning of the process may be attributed to the availability of the number of vacant or active site on the adsorbents surface which is available for the dye molecules to be occupied (Sharafzad *et al*., 2020). As the process progress beyond optimum time (90min) adsorption capacity of the adsorbents decreases slightly partly due to inaccessibility of the active site for the adsorption of MG onto surfaces of the adsorbents. Lian *et al.* (2009) reported similar results for the adsorption of Congo Red onto Ca-Bentonite. At this time, the amount of dye desorbing from the adsorbent is in state of dynamic equilibrium with the amount of dye adsorbed onto the AWL adsorbent surface.

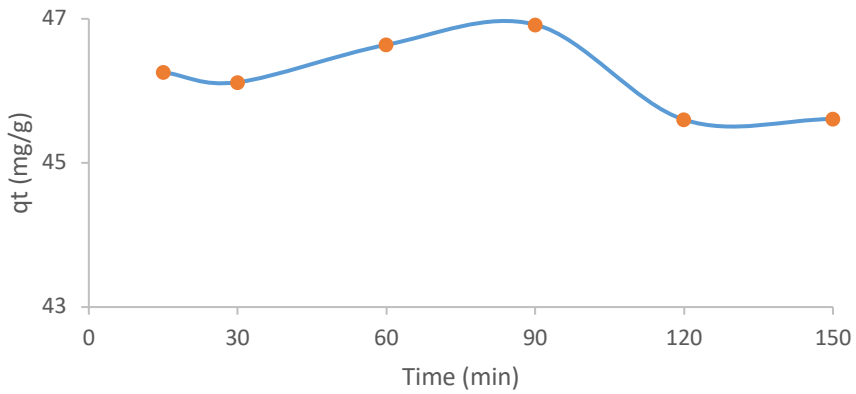

Figure 5. Effect of contact time on adsorption of MG onto AWL adsorbent

Effect of adsorbent dosage (20-200mg) on percentage removal and adsorption capacity of dye (MG) was investigated at predetermined equilibrium time (90min) and the results are demonstrated in **Figure 6**. The results show that percentage removal of dye increases (64.20% to 90.66%) as amount of adsorbents dosage increases from 20-200mg. This is partly because the number of active sites available for adsorption also increases, thus increasing the percentage adsorption of dyes. From **Figure 6**, its evident adsorption capacity of adsorbents decreases as amount of adsorbents increases and this could be partly due to overlapping or aggregation of the adsorbent active sites as the dose increases (Bedmohata *et al*., 2015).

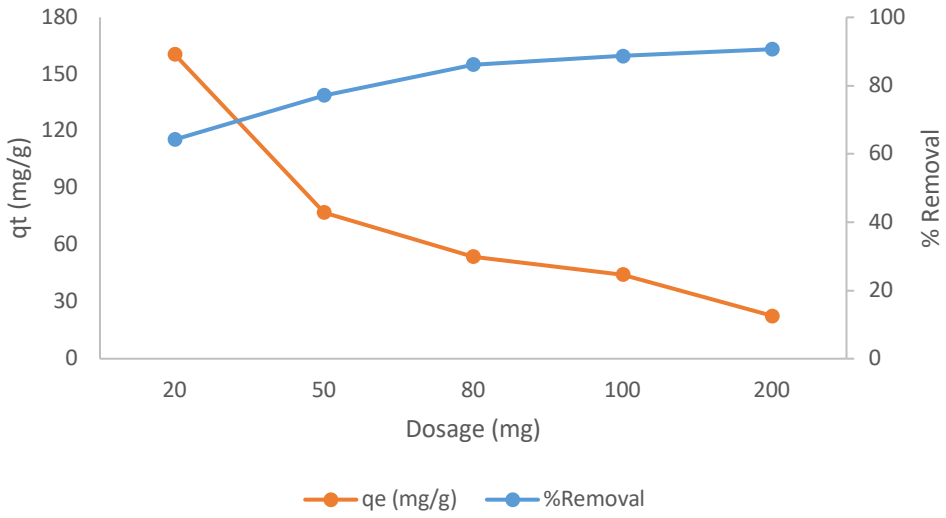

Figure 6. Effect of adsorbents dosage on adsorption of MG onto AWL adsorbent

The effect of initial concentration of MG onto AWL was investigated by varying the initial concentration of the dye from 20-120mg/L. It can be observed from **Figure 7** that adsorption capacity increased as the initial concentration increase. This is probably due to high driving forces which overcome mass transfer resistance at higher concentration of the dyes (Enenebeaku *et al*., 2016). This enhances the interaction between the adsorbates and adsorbents, as a result there was increase in dye uptakes and as such adsorption capacity increases. Similar trends were reported elsewhere (Ayuba and Bridget, 2021; Ullah *et al*., 2021). On the other hand, percentage removal increased progressively from low concentration until it reached an optimum value and then decreases as the concentration increases. This is partly due to the fact that the vacant or active sites of the adsorbent become saturated by the MG adsorbates.

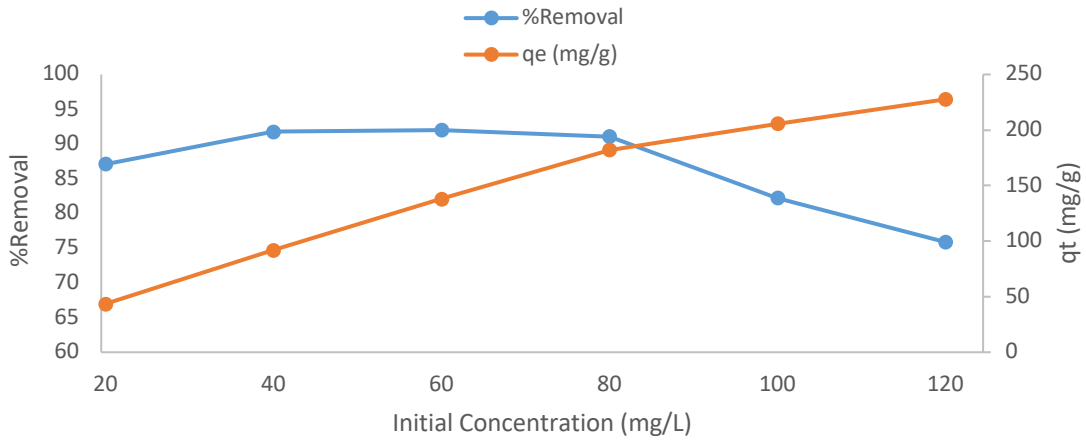

Figure 7. Effect of initial concentration on adsorption of MG onto AWL adsorbent

The effect of pH on adsorption of MG onto AWL adsorbent was studied and reported in **Figure 8.** The pH varied from 3-13 by adjusting pH of the system solution with 0.10M NaOH and or 0.10M HCl respectively. MG is a cationic dye which gives positive charge when in solution. The positive charge surface of the adsorbent in acidic medium tend to compete with excess H^+ ions in the adsorption of MG which result in low adsorption of the dye. However, there was significant improvement on the adsorption as the pH of the solution increase with slight decrease at pH=7. At pH>7 dye uptake by the adsorbent increases implying that the process is probably an electrostatics interaction. Similar trends were reported by other researchers (Han *et al*., 2014; Pathania *et al*., 2017).

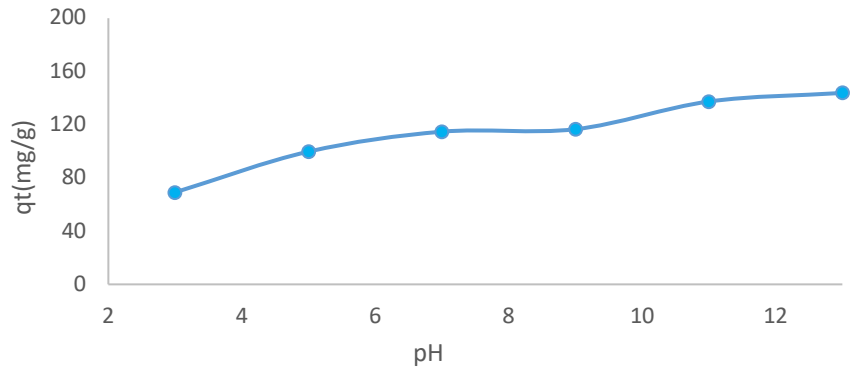

Figure 8**.** Effect of pH on adsorption of MG onto AWL adsorbent

3.4 Adsorption isotherms

Adsorption isotherm models are fundamentals for describing the behaviour of adsorbent-adsorbate interaction and also for investigation the mechanism of adsorption (Bonetto *et al*., 2015). In this study, equilibrium data was analysed using Langmuir, Freundlich, Temkin and D-R isotherm models:

(a) Langmuir Isotherm

This model is described mathematically by **Eqn. 9** (Abdu-salam and Adekola, 2018).

$$\frac{1}{q_e} = \frac{1}{q_o} + \frac{1}{q_o K_L C_e} \qquad \text{Eqn. 9}$$

Where, C_e is the equilibrium concentration of MG (mg/L), q_e is the amount of MG adsorbed at equilibrium (mg/g), q_0 is the monolayer adsorption capacity (mg/g) and K_L (mg/g) is expressed as the Langmuir constant.

The R_L factor is defined based on **Eqn. 10** (Bonetto *et al*., 2015):

$$R_L = \frac{1}{1+K_L C_0} \qquad \text{Eqn. 10}$$

The adsorption process is irreversible when R_L is 0.00, favourable when R_L is between 0.0 and 1.0, linear when R_L is equal to 1.0 and unfavourable when R_L is greater than 1.0. The values of q_o, K_L and R_L are computed and tabulated in Table 3 from slope and intercept of a plot of $1/q_e$ against $1/C_e$ respectively (graph not shown).

(b) Fruendlich Isotherm

The equilibrium concentrations of MG obtained were subjected to Freundlich isotherm equation as shown in **Eqn. 11** (Dehgani *et al*., 2018):

$$logq_e = logK_F + \frac{1}{n} logC_e \qquad \text{Eqn. 11}$$

Where K_f is the Freundlich constant demonstrating multilayer adsorption capacity and n indicates the adsorption intensity and binding energy. The values of K_f and n can be determined from intercept and slope of plot $logq_e$ against $logC_e$. If n = 1, then the partition between the two phase are independent of the dye concentration. If the values of 1/n are less than 1, it indicates normal adsorption process whereas the value of 1/n is greater than 1. Its indicate cooperative adsorption process. Therefore, the values of K_F and 1/n are computed and tabulated in **Table 3** from slope and intercept of a plot $logq_e$ against $logC_e$ respectively (graph not shown).

(c) Temkin Isotherm

This model considers the interaction between adsorbent materials and adsorbate molecules to be adsorbed and is assuming that free energy of adsorption process is a function of the surface coverage (Nyijime and Ayuba, 2020). It is expressed by **Eqn. 12**:

$$q_e = \frac{RT}{b_T} \ln A_T + \frac{RT}{b} \ln Ce \qquad \text{Eqn. 12}$$

Where $\beta = RT/b$ is related to the heat of adsorption, R is molar gas constant ($Jmol^{-1}K^{-1}$), T is temperature in Kelvin, b is variation of adsorption energy (J/mol), b_T is the equilibrium binding constant (L/mg) corresponding to the maximum binding energy. The values of β, A_T are computed and tabulated in **Table 3** from slope and intercept of q_e against lnC_e plot respectively (graph not shown).

(d) D-R isotherm

This model is used to determine the adsorption behaviour of MG towards the adsorbent using **Eqn. 13** (Nica *et al*., 2020):

$$\ln q_e = \log q_0 - K \in^2 \qquad \text{Eqn. 13}$$

Where q_o is representing the constant of D-R (mol/g), and K is the mean free energy of adsorption (kJ/mol). However, ϵ can be calculated using Eqn. 14:

$$\epsilon = RTln(1 + \frac{1}{C_e}) \qquad \text{Eqn. 14}$$

Where C_e is the adsorbate equilibrium concentration, R is the ideal gas constant (8.314J/mol.K) and T is the temperature in Kelvin. The values of q_o and K were calculated and tabulated in **Table 3** using slope and intercept from the plot of lnq_e against ϵ^2 respectively (graph not shown).

Table 3. Adsorption isotherm parameters

Isotherms	Parameters	Values
Langmuir	q_0 (mg/g)	1250
	K_L(L/mg)	0.018
	R_L	0.321
	R^2	0.7906
Freundlich	1/n	0.5596
	n	1.787
	K_F	42.560
	R^2	0.7319
Temkin	A_T	1.157
	B	69.410
	R^2	0.8824
D-R	q_o(mg/g)	230.58
	$\beta(mol^2/kJ^2)$	$2.0x10^{-6}$
	ϵ (kJ/mol)	0.084
	R^2	0.9866

From **Table 3**, the isotherms data were screened by four common isotherm models viz Langmuir, Freundlich, Temkin and D-R models. The selection of the best fit was decided only by linear regression coefficient (R^2) obtained for each model. The obtained values of R^2 (0.9866) suggested that the adsorption process at equilibrium was well fitted into D-R model compared to Langmuir, Freundlich and Temkin model with R^2 values 0.7906, 0.7319 and 0.8824 respectively under a wide range of initial concentration. The order of the fit is:

D-R > Temkin > Langmuir > Freundlich.

3.5 Kinetic studies

The study of adsorption kinetic of MG onto AWL can provide an important information on the adsorption rate and the factors affecting it. For this study, contact time of adsorption was varied from 5 to 60 minutes with an interval of 5 minutes, while other operating parameters were kept at optimized condition at temperature of 30, 40, 50^0C respectively. Pseudo first order, pseudo second order, Elovich and intraparticle diffusion models were employed to analyse the kinetic of MG onto the AWL adsorbent:

(a) Pseudo first order kinetic model

The pseudo first order equation is usually expressed as in **Eqn. 15** (Pan and Zhang, 2009):

$$\log(q_e - q_t) = \log q_e - \frac{k_1 t}{2.303} \qquad \text{Eqn. 15}$$

Where k_1 is the first order rate constant and q_e and q_t are the amount of MG adsorbed at equilibrium and time t (mg/g) respectively. The low values of R^2 and large difference between experimental adsorption capacities (q_e) at 303, 313 and 323K of 148.85, 147.48, and 145.14mg/g and calculated adsorption capacities (q_e) at 303, 313 and 323K of 1.07, 1.07 and 2.99 mg/g respectively shows that this model fails to accurately interpret the experimental data.

(b) Pseudo-second kinetic models

The pseudo second order adsorption kinetic rate equation is expressed as shown in **Eqn. 16**:

$$\frac{1}{q_t} = \frac{1}{k_2 q_e^2} + \frac{t}{q_e} \qquad \text{Eqn. 16}$$

Where k_2 is the rate constant of pseudo second order adsorption (g/mg.min). Fitting the kinetic parameters of MG onto AWL based on pseudo-second order model equation are computed and reported in **Table 4**. From the results, pseudo-second-order kinetic model fits the experimental data very well; where R^2 values are close to unity and the experimental and calculated adsorption capacities are in good agreement. This indicates the applicability of this model to describe the adsorption process of MG onto AWL adsorbent at all experimental conditions tested.

(c) Elovich Model

The Elovich kinetic model is described by **Eqn. 17**:

$$q_t = \frac{1}{\beta}\ln(\alpha\beta) + \frac{1}{\beta}\ln t \qquad \text{Eqn. 17}$$

This model gives useful information on the extent of both surface activity and activation energy for adsorption process. The R^2 values of this model (**Table 4**) showed great deviation from linearity (not closed to unity) which reflects that this model suggested by Elovich does not fit the kinetic data very well.

Table 4. Kinetics parameters of adsorption of MG onto AWL adsorbents

Temperature (K)	**Parameters**			
Pseudo-First Order	Q_{exp}*(mg/g)*	Q_{cal} *(mg/g)*	K_1*(min^{-1})*	R^2
303	148.85	1.07	1.240×10^{-2}	0.2893
313	147.48	1.07	5.30×10^{-3}	0.0227
323	145.14	2.99	1.27×10^{-2}	0.0542
Pseudo-Second Order	Q_{exp}*(mg/g)*	Q_{cal} *(mg/g)*	K_2*(g/mg.min)*	R^2
303	148.85	147.06	2.89×10^{-2}	0.9996
313	147.48	144.93	5.29×10^{-2}	0.9998
323	145.14	142.86	2.45×10^{-2}	0.9993
Elovich Model		*B*	*A*	R^2
303		1.389	0.724	0.2057
313		5.540	0.181	0.0218
323		0.660	1.532	0.3179
Intraparticle Diffusion		*C*	K_{int}	R^2
303		143.50	0.3522	0.2629
313		145.98	0.0192	0.0013
323		139.43	0.5561	0.2289

(d) Intraparticle Diffusion model

Possibility of involvement of intra particle diffusion model as the sole mechanism was investigated according to Weber-Moris **Eqn. 18** (Ogugbue and Sawidis, 2011):

$$q_t = C + k_{int} t^{1/2} \qquad \text{Eqn. 18}$$

the constant k_{int} (mg/g.min) is the intra particle diffusion rate and C is the boundary layer thickness. If the rate limiting step is only due to intra particle diffusion, then q_t vs $t^{1/2}$ will be linear and the plot passes through the origin, therefore, other mechanism along with intra-particles diffusion mechanism might involve. Since the plot of q_t against $t_{1/2}$ does not pass through the origin depending on the low R^2 determined as can be seen from the **Table 5**. It can be concluded that intra particle diffusion is not the rate determining step of the adsorption mechanism of MG adsorption onto AWL adsorbent.

3.5 Thermodynamics studies

To examine the effect of temperature on adsorption of MG onto AWL adsorbent, thermodynamics parameters such as Gibb's free energy change (ΔG), was estimated using **Eqns. 19 and 20** respectively at various experimental temperatures. Using **Eqn. 21**, a plot of $\ln K_c$ against 1/T was used to evaluate enthalpy change (ΔH) and entropy change (ΔS) values from the slope and intercept of the plot.

$$K_c = \frac{C_s}{C_e} \qquad \text{Eqn. 19}$$

$$\Delta G = -RT\ln K_c \qquad \text{Eqn. 20}$$

$$\ln K_c = -\frac{\Delta H}{RT} + \frac{\Delta S}{R} \qquad \text{Eqn. 21}$$

Table 5. Thermodynamics parameters of MG adsorption onto AWL adsorbent

T(K)	$\ln K_c$	ΔG (kJ/mol)	ΔH (kJ/mol)	ΔS (J/mol.K)
303	3.361	-8.468		
313	3.143	-8.180	-18.293	-32.593
323	2.758	-7.406		
333	2.767	-7.661		

The negative values of ΔG demonstrate the spontaneity and feasibility of the adsorption process. The decrease in its values as temperature rises shows the physical nature of the adsorption process (Idoko and Ayuba, 2020). The negative value of enthalpy change ΔH (-18.293J/mol) indicates an exothermic process (heat evolved). The magnitude of ΔH describes the type of adsorption; the heat of physical adsorption falls within the range of 2.1-20.9kJ/mol while chemisorption generally falls into higher range of 20-200kJ/mol (Abdelkreem and Hussein, 2012). The value obtained in this work fall within the range which signifies physical adsorption. The negative values of entropy ΔS (-32.593J/mol. K), suggest a decrease in randomness at the adsorbent-adsorbates interface during adsorption of MG dye ion on the adsorbent surface. This negative entropy of the dyes adsorption onto the adsorbent surface may be attributed to the decrease in the degree of freedom of the dyes molecules (Malik *et al*., 2007). Similar results were reported by other authors (Ibrahim and Jimoh, 2012; Bashir *et al*., 2013).

Conclusion

Adsorbent from water lily leaves was prepared by treating it with KOH solution. The prepared adsorbent was characterized through the determination of some of its physical and as well as structural and morphological properties. This adsorbent was used to remove Malachite green dye from aqueous solution through batch adsorption techniques. Experimental parameters including solution pH, adsorbent dosage, initial dye concentration, contact time were optimized and the percentage adsorption and adsorption capacity was found to be 90.66% and 148.85mg/g respectively. For the adsorption process, isotherms, kinetics and thermodynamics models were evaluated and found the process to obey D–R isotherm and pseudo second order kinetic models, while the process was found to be feasible and spontaneous. Base chemically activated water lily leaves was successfully used to remove Malachite green dye from aqueous solution through a mechanism of physical adsorption.

Acknowledgement: The technical inputs of the staff of Central Laboratory Complex, Bayero University, Kano are acknowledged.

Disclosure statement: *Conflict of Interest:* The authors declare that there are no conflicts of interest.
Compliance with Ethical Standards: This article does not contain any studies involving human or animal subjects.

References

Abdelkreem M. and Husein Z. D. (2012) Removal of Strontium from aqueous solution by adsorption onto orange peel: isotherms, kinetics & thermodynamics studies. *Eurasian Journal of Educational Research,* 1, 42-61.

Abdus-Salam N. and Adekola S. K. (2018) Adsorption studies of zinc (II) on magnetite, baobab (*Adensonia digitata)* & magnetite-baobab composite, *Applied Water Sciences,* 8(8), 1-11. https://doi.org/10.1007/s13201-018-0867-7.

Akartasse N., Azzaoui K., Mejdoubi E., Hammouti B., Elansari L.L., Abou-salama M., Aaddouz M., Sabbahi R., Rhazi L. and Siaj M. (2022) Environmental-Friendly Adsorbent Composite Based on Hydroxyapatite/Hydroxypropyl Methyl-Cellulose for Removal of Cationic Dyes from an Aqueous Solution, Polymers, 14(11), 2147; https://doi.org/10.3390/polym14112147

Amode O. J., Santos H. J., Alam M. Z., Mirza H. A. and Mei C. C. (2016) Adsorption of methylene Blue from aqueous solution using untreated and treated (Metroxylon spp) waste adsorbents: equilibrium and Kinetic studies, *International Journal of Industrial Chemistry,* 7, 333-345. https://doi.org/10.1007/s40090-016-0085-9.

Anisuzzaman S. M., Joseph G. C., Daud A. M. S. B. W., Krishnaiah D. and Yee H. S. (2014) Preparation and characterization of activated carbon from typha orientalis leaves, *International Journal of Industrial Chemistry*, 6, 9-21. https://doi.org/10.1007/s40090-014-0027-3.

Ayuba A. M. and Bridget I. (2021) Cowpea husk adsorbent for the removal of crystal violet dye from aqueous solution, *Arabian Journal of Chemical Research.* 8(1), 114-132.

Ayuba A. M. and Nyijime T. A. (2019) Paraquat dichloride adsorption from aqueous solution using carbonised Bambara groundnut (vigra subterranean) shells, *Bayero journal of pure and applied sciences,* 12(1), 167-177. ISSN 2006-6996. https://doi.org/10.4314/bajopas.v12i1.28S.

Ayuba A. M. and Nyijime T. A. (2021) Adsorption and kinetics study for the removal of pendimethalin from aqueous solution using activated carbon prepared from agricultural waste, *Journal of Experimental Research*, 9(2), 6-16.

Bashir A. D., Taher A., Wani A. and Farooqui M. (2013) Isotherms & thermodynamic studies on adsorption of copper on powder of shed pods of Acacia nilotica, *Journal of Environmental Chemistry and Ecotoxicology*, 5(2), 17-20. https://doi.org/10.5897/JECE12.013.

Bedmohata M. A., Chaudhari A. R., Singh S. P., Choudhary M. D. (2015) Adsorption capacity of activated carbon prepared by chemical activation of Lignin for the removal of methylene blue dye, *International Journal of advanced Research in Chemical Science (IJARCS),* 2(8), 1-13.

Bello S.O, Ahmad A. M. and Ahmad N. (2012) Adsorption features of banana (musa paradisiaca) stalk-based activated carbon for malachite green dye removal, *Chemistry & Ecology,* 28(2), 153-167. https://doi.org/10.1080/02757540.2011.628318.

Bharathi K.S. & Ramesh S.P.T. (2013) Fixed-bed column studies on biosorption of crystal violet from aqueous solution by citrullus lanatus (watermelon) rind and cyperus rotundus, *Applied Water Sciences,* 3, 673-687. https://ui.adsabs.harvard.edu/link_gateway/2013ApWS....3..673B/doi:10.1007/s13201-013-0103-4

Bonetto L. R., Ferarini F., DeMarco C., Crespo J. S., Guegun R. and Giovanela M. (2015) Removal of methyl violet 2B dye from aqueous solution using a magnetic composite as adsorbent, *Journal of water process Engineering*, 6, 11-20. https://doi.org/10.1016/j.jwpe.2015.02.006.

Crini G. (2006) Non-conventional low-cost adsorbents for the dye removal: A review, *Bioresources Technology,* 97, 1061-1085. https://doi.org/10.1016/j.biortech.2005.05.001.

Dehgani M. H., Tajik S., Panahi A., Khezri M., Zarei A., Heidarinejad A. and Yousefi M. (2018) Adsorptive removal of noxious cadmium from aqueous solution using polyureaformaldehyde: a novel polymer adsorbent, *MethodsX,* 5, 1148-1155. https://doi.org/10.1016/j.mex.2018.09.010.

Elsherif K. M., El-Dali A., Ewlad-Ahmed A. M., Treban A. A., Alqadhi H. and Alkarewi S. (2022) Kinetics and isotherms studies of safranin adsorption onto two surfaces prepared from orange peels, *Moroccan Journal of Chemistry*, 10(4), 639-651. https://doi.org/10.48317/IMIST.PRSM/morjchem-v11i1.32137.

Enenebeaku K. C., Okorocha J. N., Enenebeaku E. U., Okolie I. J. and Anukum B. (2016) Adsorption of malachite green from aqueous solution by PNSBP: equilibrium, kinetic and thermodynamics studies, *IOSR Journal of applied Chemistry*, 9 (9), e-ISSN: 2278-5736 28-38.

Erradi E. M. and Jaafari K. (2022) Study of dechlorination by natural adsorbents (chitin and chitosan), *Moroccan Journal of Chemistry*, 10(2), 218-234. https://doi.org/10.48317/IMIST.PRSM/morjchem-v9i3.21865.

Gaya U. I., Otene E. and Abdullahi A. H. (2015) Adsorption of aqueous Cd (II) and Pb(II) on activated carbon nanopores prepared by chemical activation of doum palm shell, *SpringerPlus*, 4, 458. https://doi.org/10.1186/s40064-015-1256-4.

Giwa S. O., Moses J. S., Adeyi A. A. and Giwa A. (2018) Adsorption of atrazzine from aqueous solution using desert date seed shell activated carbon, ABUAD *Journal of Engineering Research & Development (AJERD)*, 1(3), 317-325.

Han X., Yuan J. and Ma X. (2014) Adsorption of malachite green from aqueous solutions onto lotus leaf: equilibrium, kinetics and thermodynamics studies, *Desalination and water Treatment*, 52(2), 5563-5574. https://doi.org/10.1080/19443994.2013.813102.

Ibrahim M. B. and Jimoh W. L. O. (2008) Adsorption studies for the removal of Cr (VI) ions from aqueous solutions, *Bayero Journal of Pure and Applied Sciences,* 1(1), 99-103. https://doi.org/10.4314/bajopas.v1i1.57519.

Ibrahim M. B. and Jimoh W. L. O. (2012) Thermodynamics and adsorption isotherms for biosorption of Cr(VI), Ni (II), & Cd(II) onto maize cobs, *ChemSearch Journal,* 3(1), 7-12. https://www.ajol.info/index.php/csj/article/view/115714.

Ibrahim M. B. and Sani S. (2015) Neem (*Azadirachta Indica*) leaves for the removal of organic pollutants, *Journal of Geosciences and Environmental protection,* 3, 1-9. http://dx.doi.org/10.4236/gep.2015.32001.

Idoko B. and Ayuba A. M. (2020) Kinetics, equilibrium & thermodynamics studies on adsorption of crystal violet dye from aqueous solution using activated cowpea (*Vigna unguiculata)* Husk, *Applied Journal of Environmental Engineering Sciences,* 6(2), 182-195. *https://doi.org/10.48422/IMIST.PRSM/ajees-v6i2.20984*.

Kali A., Dehmani Y., Loulidi I., Amar A., Jabri M., El-kord A. and Boukhlifi F. (2022) Study of the adsorption properties of an almond shell in the elimination of methylene blue in an aquatic, *Moroccan Journal of Chemistry*, 10(3), 509-522. https://doi.org/10.48317/IMIST.PRSM/morjchem-v10i3.33140.

Kankou M. S.'A., N'diaye A. D., Hammouti B., Kaya S. and Fekhaoui M. (2021) Ultrasound-assisted adsorption of Methyl Parathion using commercial Granular Activated Carbon from aqueous solution, *Mor. J. Chem.* 9(4), 832-842

Kihc M. and Janabi A. S. K. (2017) Investigation of dyes adsorption with activated carbon obtained from cordia myxa, *Bilge International Journal of Science and Technology Research,* 1(2), 87-104. https://dergipark.org.tr/en/pub/bilgesci/issue/32353/341906.

Lian L., Gua L. and Gua C. (2009) Adsorption of congo red from aqueous solution on cabentonite. *Journal of Hazardous Materials,* 161, 126-131. https://doi.org/10.1016/j.jhazmat.2008.03.063.

Mafra I. L., Mafra M. R., Zuim D. R., Vaques E. C. and Ferreira A. M. (2013) Adsorption of remazol brilliant blue on orange peel as adsorbents, *Brazilian Journal of Chemical Engineering,* 30(3), 657-665. https://doi.org/10.1590/S0104-66322013000300022.

Makeswari, M. and Santhi T. (2013) Optimization of preparation of activated carbon from Ricinus communis Leaves by microwave-assisted zinc chloride chemical activation: competitive adsorption of Ni^{2+} ions from aqueous solution, *Journal of Chemistry,* 1-13. https://doi.org/10.1155/2013/314790.

Malik R., Ramteke D. S. and Wate S. R. (2007) Adsorption of malachite green on groundnut shell waste based powdered activated carbon, *Waste Management,* 29(9), 129-138. https://doi.org/10.1016/j.wasman.2006.06.009.

Marczewski A. W., Seczkowska M., Deryło-Marczewska A. and Blachnio M. (2016) Adsorption equilibrium and kinetics of selected phenoxyacid pesticides on activated carbon: effect of temperature, *Adsorption*, 22(4), 777-790. https://doi.org/10.1007/s10450-016-9774-0.

Monvisade P. and Siriphannon P. (2009) Chitosan intercalated montmorillonite: preparation, characterization & cationic dye adsorption, *Applied Clay Sciences,* 42, 427-431. https://doi.org/10.1016/j.clay.2008.04.013.

Nasiruddin K. M. and Sawar A. (2007) Determination of point of charge of natural and treated adsorbents, *Surface Review and Letters,* 14(3), 461-469. https://doi.org/10.1142/S0218625X07009517.

Nica I., Zaharia C., Baron R. I., Coseri S. and Suteu D. (2020) Adsorptive materials based on preparation, characterization and application of copper ion retention, *Cellulose Chemistry Technology,* 54(5-6), 579-590. http://dx.doi.org/10.35812/CelluloseChemTechnol.2020.54.58.

Nyijime T. A. and Ayuba A. M. (2020) Kinetics and equilibrium studies of paraquat dichloride adsorption on raw bambara groundnut (*vigna subteranean) shells*, *Applied Journal of Environmental Engineering Sciences,* 6(1), 1-13. *https://doi.org/10.48422/IMIST.PRSM/ajees-v6i1.19487*.

Nyijime T. A., Ayuba A. M. and Chahul H. F. (2021) Removal of pendimethalin from aqueous solution by carbon prepared from bambara groundnut (*Vigna subteranean*) Shells, *Arabian Journal of Chemical and Environmental Research,* 8(2), 315–335**.**

Ogugbue C. J. and Sawidis T. (2011) Bioremediation and detoxification of synthetic wastewater containing triarylmethane dyes by Aeromonas hydrophila isolated from industrial effluents, *Biotechnology Research International,* 16, 167-169. https://doi.org/10.4061/2011/967925.

Ojediran J.O., Dada A. O., Aniyi S. O., David R. O., Adewumi A. D. (2021) Mechanism and isotherm modelling of effective adsorption of malachite green as endocrine disruptive dye using Acid Functionalized Maize Cob (AFMC), *Scientific Reports,* 11, 21498. https://doi.org/10.1038/s41598-021-00993-1.

Oznur D., Fatma I., Kadir T. and Mahmure O. (2013) Sumec leaves as a novel low cost adsorbent for removal of basic dyes from aqueous solution, *Hindawi publishing corporation (ISRN) analytical Chemistry,* Article ID. 1210470, 1-9. http://dx.doi.org/10.1155/2013/210470.

Pan X. and Zhang D. (2009) Removal of malachite green from water by firmiana simplex wood fiber, *e-Journal of biotechnology,* 12(4), ISSN: 0177-3458. http://dx.doi.org/10.4067/S0717-34582009000400009.

Pathania D., Sharma S. and Singh P. (2017) Removal of methylene blue by adsorption onto activated carbon developed from *Ficus carica bast*, *Arabian Journal of Chemistry*, 10(1), S1445-S1451. https://doi.org/10.1016/j.arabjc.2013.04.021,

Sartape S. A., Mandhare M. A., Jadhav V. V., Raut D. P., Anusa A. M. and Kolekar S. S. (2017) Removal of malachite green dye from aqueous solution with sorption techniques using *Limonia Acidissima* (wood apple) Shell as low cost adsorbents, *Arabian Journal of Chemistry,*10, 3229-3238. https://doi.org/10.1016/j.arabjc.2013.12.019.

Sciban M., Klasnja M. and Skrbic B. (2008) Adsorption of copper ion from water by modified agricultural by-product, *Desalination,* 229, 170-180. https://doi.org/10.1016/j.desal.2007.08.017.

Shahryari Z., Goharrizi S. A. and Azadi M. (2010) Experimental study of methylene blue adsorption from aqueous solution onto a carbon nano tubes, *International Journal of water Resources and environmental engineering,* 2(2), 016-028.

Sharafzad A., Tamjidi S. and Esmaeili H. (2020) Calcined lotus leaf as a low cost and highly efficient adsorbent for the removal of methyl violet dye from aqueous media, *International Journal of Environmental analytical chemistry,* https://doi.org/10.1080/03067319.2020.1711894.

Suyambo B. K. and Perumel R. S. (2012) Equilibrium, thermodynamics and kinetics studies on adsorption of basic dye by Citrullus lanatus rind, *Iranica Journal of Energy and Enviroment,* 3(1), 23-34.

Tcheka C., Abia D., Iya-sou D. and Tamgue A. T. (2021) Removal of crystal violet dye from aqueous solutions using chemically activated carbons by H3PO4 activation from corn cobs and corn roots: kinetic and equilibrium isotherm studies, *Moroccan Journal of Chemistry*, 9(2), 221-231. https://doi.org/10.48317/IMIST.PRSM/morjchem-v9i2.22099.

Ullah S., Ur Rahman A., Ullah F., Rashid A., Arshad T., Viglasova E., Galambos M., Mahmoode M. N. and Ullah H. (2021), Adsorption of Malachite green dye onto mesoporous natural inorganics clays: equilibrium isotherm and kinetic studies, *Water,* 13(7), 965. https://doi.org/10.3390/w13070965.

Zendegani A. and Shokrollahi A. (2014) Adsorption of violet covasol dye from aqueous solution with Nymphaea alba: Kinetic and Thermodynamics study ", *17th Iranian Chemistry Congress Vali e-Asr University of Rafsanjani,* 1-3.

(2023) ; https://revues.imist.ma/index.php/morjchem/index